Electronic Structure of the Si(111)2×1 Surface by Scanning-Tunneling Microscopy

Joseph A. Stroscio, R. M. Feenstra, and A. P. Fein
IBM Thomas J. Watson Research Center, Yorktown Heights, New York 10598
(Received 30 June 1986)

The tunneling current is measured as a function of voltage, lateral position, and vertical separation between a tungsten probe tip and a Si(111)2×1 surface. A rich spectrum is obtained in the ratio of differential to total conductivity, revealing the structure of the surface-state bands. The magnitude of the parallel wave vector for certain surface states is determined from the decay length of the tunneling current. Real-space images of the surface states reveal a phase reversal between those states on either side of the surface-state band gap.

PACS numbers: 73.20.Cw, 61.16.Di, 68.35.Bs

The band structure of the Si(111)2×1 surface has been studied by a variety of experimental techniques. Optical absorption[1] first revealed the presence of two surface bands, separated by an energy gap of about 0.45 eV. The dispersion of the lower band and part of the upper band has been observed by angle-resolved photoemission[2-4] and inverse photoemission.[5] The dispersion of the observed bands is in good agreement with that predicted theoretically[6,7] with use of the π-bonded chain model of this 2×1 reconstructed surface. This agreement, together with the results of other structure-sensitive techniques, provides strong support for the π-bonded chain model as the correct structure of the Si(111)2×1 surface.

In this work, we use the technique of scanning-tunneling microscopy (STM)[8] to determine the electronic properties of the Si(111)2×1 surface. Spectroscopic measurements by STM consist essentially of bringing of a metal probe tip 5–15 Å away from a sample surface, application of a voltage between tip and sample, and measurement of the resulting tunneling current. The differential conductivity, dI/dV, provides a direct measure of the surface density of states (DOS).[9] Our results presented here provide the first determination of a surface DOS over the entire energy range -4 to 4 eV relative to the Fermi level (outside this range the spectrum is dominated by barrier resonances[8,10]). The DOS we obtain shows the structure of the two π-bonding surface-state bands, together with a newly identified surface resonance at 2.3 eV above the Fermi level. We have performed, for the first time, spectroscopic measurements at various values of the separation between probe tip and sample, thereby obtaining a measure of the magnitude of the parallel wave vector of those states which participate in the tunneling process. A parallel wave vector of about 1.1 $Å^{-1}$ is observed for states with energies near the surface band gap, indicating their origin from the edge of the surface Brillioun zone. STM images of states on either side of the gap reveal a phase reversal (180° phase shift) in the $[01\bar{1}]$ corrugation, indicating a parity reversal of the wave functions across the band gap.

The tunneling microscope used here is similar to that described by Binnig and Rohrer,[8] and is described in detail elsewhere.[11] The microscope is contained in an ultrahigh-vacuum chamber with an operating pressure of $<4\times10^{-11}$ Torr. The Si (111) surfaces were prepared by *in situ* cleaving. Both n- and p-type material with resistivities ranging from 0.005–5 Ω-cm have been studied. The current-voltage (I-V) curves presented here were obtained from a 5-Ω-cm n-type sample. The results are practically independent of doping, with the exception that a small voltage shift in the entire I-V spectrum is observed in the highly doped material. We attribute this shift to a change in the surface Fermi-level position in accordance with that observed by other authors.[4] Tungsten probe tips prepared by electrochemical etching were used. The I-V measurements were performed with a constant separation between probe tip and sample, obtained by use of a sample-and-hold circuit in the STM feedback loop.[11]

Our spectroscopic results are presented in Fig. 1. In

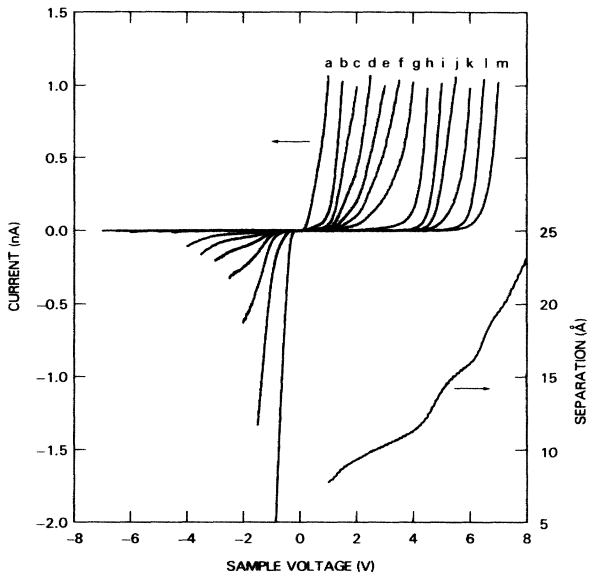

FIG. 1. Tunneling current vs voltage (I-V) for a tungsten probe tip and Si(111)2×1 sample, at tip-sample separations of 7.8, 8.7, 9.3, 9.9, 10.3, 10.8, 11.3, 12.3, 14.1, 15.1, 16.0, 17.7, and 19.5 Å for the curves labeled a–m, respectively. These separations are obtained from a measurement of separation vs voltage, at 1-nA constant current, shown in the lower part of the figure.

the upper panel we plot a sequence of I-V curves, obtained at constant values of the tip-sample separation. A plot of the separation versus voltage (s-V), at a constant current of 1 nA, is shown in the lower part of the figure. Above 4 V the s-V curve displays oscillations which are due to barrier resonances.[8,10] By matching the observed s-V curve with theoretical computations[12] similar to those described in Ref. 10, we find an average work function of 4.5 eV between tip and sample, and we approximately determine the zero of separation. As seen in Fig. 1, the barrier resonances give rise to gaps between the I-V curves, e.g., between curves g and h, and between j and k. We also observe a rectifying behavior of the data in Fig. 1. In a given I-V curve, this behavior appears as a larger current at positive voltage than at negative voltage. This same behavior is observed in both n- and p-type material, independent of doping, so that the effect does not arise from band bending in the semiconductor. We find that the observed rectifying behavior can be quantitatively accounted for by an enhancement of the electric field in the junction as a result of the finite probe-tip radius of curvature. Computations of this effect are presented elsewhere.[12]

By acquiring I-V curves at various values of the tip-sample separation, we obtain measurements of the current as a function of separation at constant voltage. Fitting these measurements by exponentials, we determine the inverse decay length of the tunneling current, shown in Fig. 2(a). In the simplest approximation the inverse decay length equals $2[2m\bar{\phi}/\hbar^2]^{1/2} \simeq 2.2$ Å^{-1} where $\bar{\phi}$ is the average work function and m is the free-electron mass. This value is close to that which we observe at energies with magnitude greater than 1 eV. At energies closer to zero, the inverse decay length increases sharply. We attribute this increase to tunneling from states with large values of parallel wave vector. Current arising from a state with parallel wave vector $k_\parallel$ will decay into the vacuum with an inverse decay length of[9] $2[(2m\bar{\phi}/\hbar^2)+k_\parallel^2]^{1/2}$. Using this formula, we find a value of $k_\parallel \simeq 1.1$ Å^{-1} for the states near zero energy, which is close to the maximum wave vector at the edge of the surface Brillouin zone ($\bar{K}$ point) of 0.94 Å^{-1}. Thus, at energies with magnitude less than 1 eV, tunneling is occurring through states located near the edge of the Brillouin zone, and at higher energies states near the center of the zone dominate the tunneling current.

Density-of-states features in the I-V curves of Fig. 1 appear as the various kinks and bumps occurring between -4 and 4 V. These features are obscured by the fact that the tunneling current depends exponentially on both separation and applied voltage. Most of this dependence can be removed by computation of the ratio of differential to total conductivity, $(dI/dV)(I/V)^{-1}$, which provides a relatively direct measure of the surface DOS.[9,12,13] The results of such an analysis, applied to the data of Fig. 1, are shown in Fig. 2(b). There, each type of data symbol refers to a different curve (i.e., different tip-sample separation) from Fig. 1. We see that the results are practically independent of separation, thus providing a convenient "invariant" quantity.

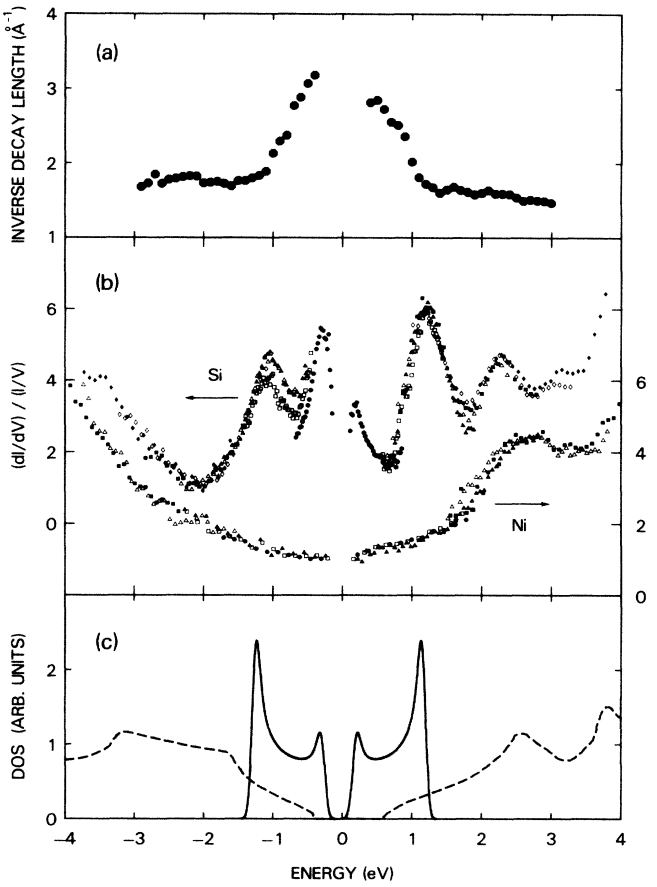

FIG. 2. (a) Inverse decay length of the tunneling current as a function of energy (relative to the Fermi level). (b) Ratio of differential to total conductivity for silicon and for nickel. The different symbols refer to different tip-sample separations. For silicon, the circles, open squares, filled triangles, open triangles, filled squares, open lozenges, and filled lozenges refer to the curves a–g, respectively, from Fig. 1. (c) Theoretical DOS for the bulk valence band and conduction band of silicon (dashed line, taken from Ref. 14), and the DOS from a one-dimensional tight-binding model of the π-bonded chains (solid line).

A number of peaks are evident in the spectrum of Fig. 2(b), at energies of -1.1, -0.3, 0.2, 1.2, and 2.3 eV, along with a small peak near 3.2 eV [note that the quantity $(dI/dV)(I/V)^{-1}$ by definition equals unity at $V=0$]. To identify these peaks, we plot in Fig. 2(c) theoretical DOS results. We show the bulk DOS for silicon,[14] and the surface DOS for a one-dimensional tight-binding model of π-bonded chains,[15] where the surface states are located relative to the bulk states by use of photoemission results.[16] By comparison of experiment and theory, some of the observed peaks can be immediately identified with known electronic features of the Si(111)2×1 surface: The peaks at -0.3 and 0.2 eV en-

compass the gap separating the occupied (π-bonding) and unoccupied (π^*-antibonding) bands of surface states. We observe that the -0.3-eV peak is about twice as large as the 0.2-eV peak. This enhancement probably arises from mixing between valence-band states and the surface states at the top of the occupied band. The peak at -1.1 eV corresponds to the bottom of the occupied band, and the peak at 1.2 eV corresponds to the top of the unoccupied band. We observe that the bandwidth of the occupied band (0.8 eV) is less than the bandwidth of the unoccupied band (1.0 eV), in agreement with theoretical predictions[6] for the π-bonded chain. The peak at 2.3 eV probably arises from the lowest-lying conduction band near the L point in the bulk band structure, which gives rise to a peak at $E_f+2.0$ eV in inverse photoemission.[5] Bulk states at the L point, having large wave vector in the (111) direction, will contribute significantly to the formation of (111) surface states. Thus, we argue that the top of the unoccupied surface band is a two-peaked resonance, with one peak at 1.2 eV corresponding to the natural energy of the π-bonded chains, and the other peak at 2.3 eV corresponding to a strong resonance with the bulk states of the lowest-lying conduction band at the L point. A similar explanation could account for the features observed near bulk critical points in spectroscopic studies on metal surfaces.[17]

It is important to note that, in principle, DOS features from the tungsten probe tip could contribute to our spectroscopic observations. To evaluate this contribution we have performed spectroscopy using tungsten probe tips to study evaporated nickel films. The tungsten probes were prepared in an identical manner to those used for the silicon studies, and in some cases the same probes were used to study both materials without breaking vacuum. Typical spectroscopic results for a Ni sample are shown in Fig. 2(b). We see that the spectrum is featureless aside from a single peak at 2.7 eV. A peak at the same energy has been previously seen on Ni (100) surfaces and identified as a Ni-related surface state.[18] Thus, we find that the tungsten probe tips do not contribute any significant features to our observed spectra.

To probe the dependence of the surface-state spectrum on lateral position, we examine the voltage dependence of the STM images themselves. Figure 3(a) shows STM images of the Si(111)2×1 surface. The images are characterized by an array of maxima, with neighboring maxima separated by the unit-cell dimensions of 6.65×3.84 Å in the $[2\bar{1}1]$ and $[01\bar{1}]$ directions, respectively (note that the spatial resolution of these images is higher than previously reported,[11] presumably because of a sharper probe tip used in the present study). The images of Fig. 3(a) were acquired simultaneously at positive and negative sample biases of 0.7 V. This simultaneous acquisition was accomplished by reversal of the polarity in alternate line scans, which are separated and corrected for drift in Fig. 3(a). For reference cross-

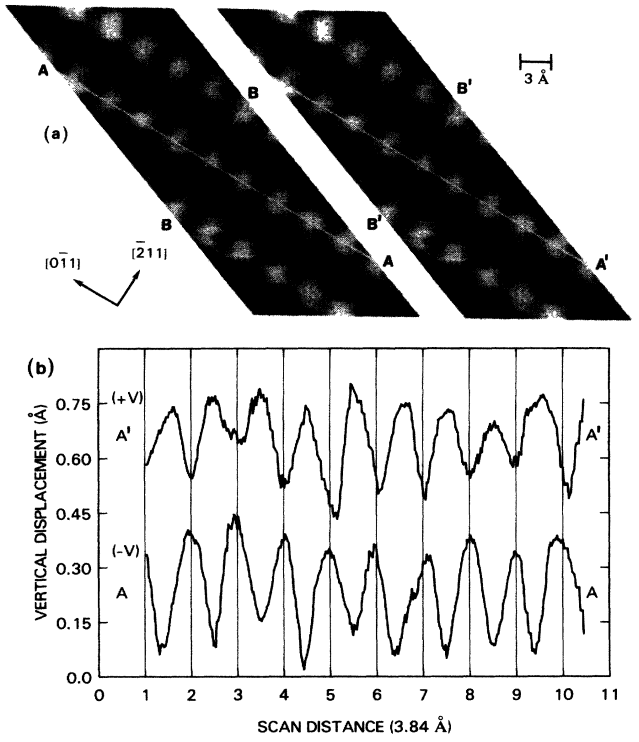

FIG. 3. (a) Constant-current STM images acquired at voltages of -0.7 and $+0.7$ V for the left and right images, respectively. The surface height is given by a grey scale, ranging from 0 Å (black) to ~1 Å (white). (b) Surface height along cross sections AA and $A'A'$, which occur at identical lateral positions in the two images. The curve $A'A'$ has been shifted 0.5 Å upwards relative to AA, and the zero level on the y axis is arbitrary. Maxima in one cross section correspond to minima in the other.

sectional cuts are displayed at the same surface location in both images. Focusing on the center of the cuts, we observe for the $[01\bar{1}]$ corrugation a maximum at negative voltage, and a minimum at positive voltage, i.e., the corrugation reverses phase. This is quantitatively displayed in Fig. 3(b) where we plot the surface height along the AA and $A'A'$ cuts, and obtain a measure of the phase shift of the $[01\bar{1}]$ corrugation of $195° \pm 15°$. The $[2\bar{1}\bar{1}]$ corrugation undergoes a small phase shift of $37° \pm 6°$ (0.68 ± 0.11 Å) under the polarity reversal, as seen in Fig. 3(a). Similar results have been obtained for voltages with magnitudes in the range 0.5–1.5 V.

The striking behavior observed in Fig. 3 indicates that the STM images are dominated by the spatial dependence of the surface-state wave functions. In the images of Fig. 3(a), we probe those states which make up the DOS peaks lying just above and just below the energy band gap, as seen in Fig. 2(b). According to the π-bonded chain model, those DOS peaks arise from states located along the $\overline{JK}$ edge of the Brillioun plane. These states have opposite parities as a result of the existence of an $[01\bar{1}]$ reflection plane. Opposite parities of the wave functions result in a phase reversal of the local

DOS, consistent with our observations. The $[01\bar{1}]$ phase reversal which we observe, along with the lack of a $[2\bar{1}\bar{1}]$ phase reversal, is precisely the same phenomena which gives rise to the highly anisotropic 0.45-eV optical absorption on this surface.[15]

In conclusion, we have shown that the ratio of differential to total conductivity obtained with the STM yields a rich spectral density of the surface electronic structure. The density of the occupied and unoccupied π-bonded surface-state bands for the Si(111)2×1 surface were observed, along with a resonance arising from a conduction-band critical point. The magnitudes of the wave vectors of these states were obtained from the dependence of the tunneling current on separation. States around the surface band gap showed an enhancement of their inverse decay length, indicating that they originate from the edge of the surface Brillioun zone. The spatial dependence of these states was examined from the phase of the corrugation in the STM images. The states on either side of the band gap are found to have opposite parities, by the observation of a phase reversal in the $[01\bar{1}]$ corrugation. This unique feature demonstrates that the STM images of this surface are dominated by the spatial dependence of the surface electronic structure, and not by the geometrical positions of the atoms.

We thank A. Baratoff for first suggesting to us the possibility of a phase reversal of the surface states, and we gratefully acknowledge discussions with N. D. Lang, K. C. Pandey, and J. Tersoff.

[1]G. Chiarotti, S. Nannarone, R. Pastore, and P. Chiaradia, Phys. Rev. B **4**, 3398 (1971).

[2]F. J. Himpsel, P. Heimann, and D. E. Eastman, Phys. Rev. B **24**, 2003 (1981).

[3]R. I. Uhrberg, G. V. Hansson, J. M. Nicholls, and S. A. Flodström, Phys. Rev. Lett. **48**, 1032 (1982).

[4]P. Mårtensson, A. Cricenti, and G. V. Hansson, Phys. Rev. B **32**, 6959 (1985).

[5]D. Straub, L. Ley, and F. J. Himpsel, Phys. Rev. Lett. **54**, 142 (1985).

[6]K. C. Pandey, Phys. Rev. Lett. **47**, 1913 (1981); Phys. Rev. Lett. **49**, 223 (1982), and Proc. Indian Natn. Sci. Acad. Part A **51**, 17 (1985).

[7]J. E. Northrup and M. L. Cohen, Phys. Rev. Lett. **49**, 1349 (1982).

[8]G. Binnig and H. Rohrer, Helv. Phys. Acta **55**, 726 (1982), and Surf. Sci. **152/153**, 17 (1985).

[9]J. Tersoff and D. R. Hamann, Phys. Rev. Lett. **50**, 1998 (1983), and Phys. Rev. B **31**, 805 (1985).

[10]R. S. Becker, J. A. Golovchenko, and B. S. Swartzentruber, Phys. Rev. Lett. **55**, 987 (1985).

[11]R. M. Feenstra, W. A. Thompson, and A. P. Fein, Phys. Rev. Lett. **56**, 608 (1986), and J. Vac. Sci. Technol. A **4**, 1315 (1986).

[12]R. M. Feenstra, J. A. Stroscio, and A. P. Fein, in Proceeding of the 1986 Scanning Tunneling Microscopy Conference, Santiago de Compostela, Spain, 14–18 July 1986, Surf. Sci. (to be published).

[13]N. D. Lang, Phys. Rev. B **34**, 5947 (1986).

[14]J. R. Chelikowsky and M. L. Cohen, Phys. Rev. B **10**, 5095 (1974).

[15]R. Del Sole and A. Selloni, Phys. Rev. B **30**, 883 (1984). We modify the DOS with a Gaussian broadening of 0.12 eV FWHM. A bandwidth of 1 eV for the upper and lower bands is chosen to match roughly theoretical dispersion curves for the π-bonded chains (Ref. 6), a band gap of 0.45 eV is chosen to match experiment (Refs. 1 and 4), and the bands are centered about −0.05 eV to match the STM results of this work.

[16]F. J. Himpsel, G. Hollinger, and R. A. Pollack, Phys. Rev. B **28**, 7014 (1983).

[17]W. J. Kaiser and R. C. Jaklevic, IBM J. Res. Dev. **30**, 411 (1986).

[18]G. Binnig, K. H. Frank, H. Fuchs, N. Garcia, B. Reihl, H. Rohrer, F. Salvan, and A. R. Williams, Phys. Rev. Lett. **55**, 991 (1985).

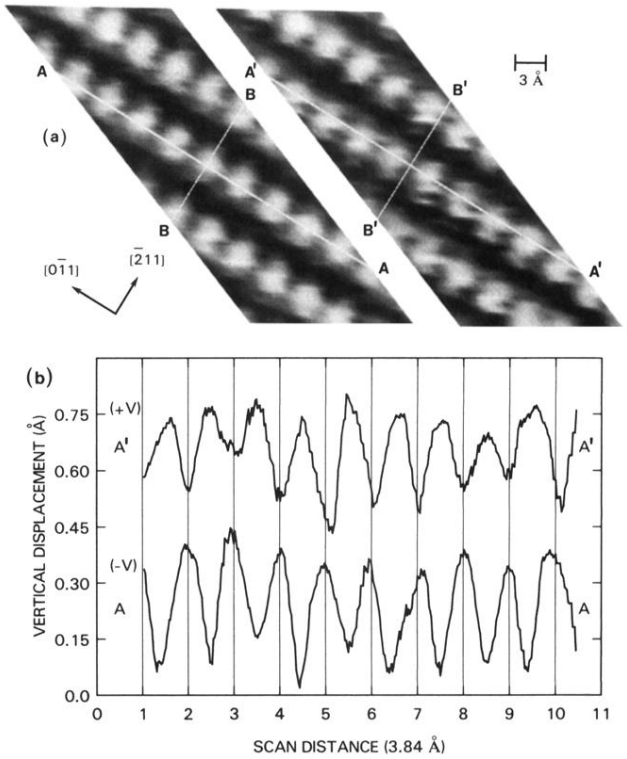

FIG. 3. (a) Constant-current STM images acquired at voltages of -0.7 and $+0.7$ V for the left and right images, respectively. The surface height is given by a grey scale, ranging from 0 Å (black) to ~ 1 Å (white). (b) Surface height along cross sections AA and $A'A'$, which occur at identical lateral positions in the two images. The curve $A'A'$ has been shifted 0.5 Å upwards relative to AA, and the zero level on the y axis is arbitrary. Maxima in one cross section correspond to minima in the other.